Solving the Dirichlet-to-Neumann map on an oblate spheroid by a mesh-free method

A. Costea[a], Q.T. Le Gia[b,*], D. Pham[c], E. P. Stephan[a]

[a]*Institut für Angewandte Mathematik and QUEST (Centre for Quantum Engineering and Space-Time Research), Leibniz Universität Hannover,Welfengarten 1, 30167 Hannover, Germany.*
[b]*School of Mathematics and Statistics, University of New South Wales, Sydney, NSW 2052,Australia.*
[c]*Institut für Numerische Simulation, Endenicher Allee 60, 53115 Bonn, Germany.*

Abstract

In this paper, we study a mesh-free method using the Galerkin method with radial basis functions (RBFs) for the exterior Neumann problem of the Laplacian with boundary condition on an oblate spheroid. This problem is reformulated as a pseudo-differential equation on the spheroid by using the Dirichlet-to-Neumann map. We show convergence of the Galerkin scheme. Our approach is particularly suitable for handling scattered data. We also propose a fast solution technique based on a domain decomposition method (obtained by the additive Schwarz operator) to precondition the ill-conditioned matrices arising from the Galerkin scheme. We estimate the condition number of the preconditioned system. Numerical results supporting the theoretical results are presented.

Keywords: mesh free method, Dirichlet-to-Neumann map, oblate spheroid

1. Introduction

In this paper, we construct numerical solutions to the Neumann problem for the Laplacian exterior to an oblate spheroid. Applications of such

*Correspoding author
Email addresses: costea@ifam.uni-hannover.de (A. Costea), qlegia@unsw.edu.au (Q.T. Le Gia), duong.pham@hcm.uni-bonn.de (D. Pham), stephan@ifam.uni-hannover.de (E. P. Stephan)

problems can be found in geophysics [3, 5], when the earth is modelled as an oblate spheroid.

There are two key ingredients in our approach: the first one is the use of the Dirichlet-to-Neumann map which directly converts the boundary value problem into a pseudodifferential equation on the spheroid. The second ingredient is the use of spherical radial basis functions (RBFs) in the Galerkin method to solve approximately this pseudo-differential equation. The advantage of using RBFs is that they enable us to handle scattered data, e.g satellite data. As a result, we prove that if the solution is smooth then a high rate of convergence of the approximate solution can be achieved by choosing appropriate RBFs.

Since the linear systems arising from our discretization are ill-conditioned, we also discuss a preconditioning strategy based on the additive Schwarz method which gives us a fast solution procedure.

The paper is organized as follows. In Section 2, we derive the pseudo-differential equation on the oblate spheroid which represents the Dirichlet-to-Neumann map. We show how to use the solution of this pseudo-differential equation to obtain the solution for the exterior Neumann problem. In Section 3, the symbol of this pseudo-differential equation is used explicitly to compute the entries of the stiffness matrix in the Galerkin scheme where we use radial basis functions. For smooth data, we give an optimal a priori error estimate for the Galerkin approximation to the exact solution. In Section 4 we introduce the additive Schwarz preconditioner and give an estimate for the condition number of the preconditioned stiffness matrix. In Section 5 we comment on the implementation with locally supported RBFs. The last section reports our numerical experiments which underly the theory.

2. The Dirichlet-to-Neumann map on the oblate spheroid

Let the oblate spheroid be given by

$$\Gamma_0 = \{(x_1, x_2, x_3) \in \mathbb{R}^3 : \frac{x_1^2}{a^2} + \frac{x_2^2}{a^2} + \frac{x_3^2}{b^2} = 1,\, a > b > 0\}$$

and Ω^c. A point $\boldsymbol{x} = (x_1, x_2, x_3) \in \mathbb{R}^3$ can be represented in oblate spheroid coordinates as

$$\begin{cases} x_1 = f_0 \cosh \mu_0 \sin\theta \cos\varphi \\ x_2 = f_0 \cosh \mu_0 \sin\theta \sin\varphi \\ x_3 = f_0 \sinh \mu_0 \cos\theta \end{cases} \tag{2.1}$$

where $\mu_0 > 0, f_0 = \sqrt{a^2 - b^2}, a = f_0 \cosh \mu_0, b = f_0 \sinh \mu_0, \theta \in [0, \pi]$ and $\varphi \in [0, 2\pi)$. In oblate spherical coordinates, the Laplace operator is written as

$$\begin{aligned} \Delta &= \frac{1}{f_0^2(\cosh^2 \mu - \sin^2 \theta)} \left\{ \frac{1}{\cosh \mu} \frac{\partial}{\partial \mu} \left(\cosh \mu \frac{\partial}{\partial \mu} \right) \right. \\ &+ \left. \frac{1}{\sin \theta} \frac{\partial}{\partial \theta} \left(\sin \theta \frac{\partial}{\partial \theta} \right) + \left(\frac{1}{\sin^2 \theta} - \frac{1}{\cosh^2 \mu} \right) \frac{\partial^2}{\partial \varphi^2} \right\}. \end{aligned}$$

Exterior to the oblate spheroid Γ_0, we consider the Neumann problem: given $g \in L_2(\Gamma_0)$, find U in the unbounded domain Ω^c outside Γ_0 satisfying

$$\begin{cases} \Delta U = 0 & \text{in} \quad \Omega^c \\ \partial_\nu U = g & \text{on} \quad \Gamma_0 \\ U(\boldsymbol{x}) = O(||\boldsymbol{x}||^{-1}) & \text{as} \quad ||\boldsymbol{x}|| \to \infty \end{cases} \tag{2.2}$$

where $||\boldsymbol{x}||$ denotes the Euclidean norm of $\boldsymbol{x}$ and ν denotes the unit outward normal vector on Γ_0. Suppose $u(\theta, \varphi) := U(\mu_0, \theta, \varphi)$ is expanded into an absolutely convergent series

$$u(\theta, \varphi) = \sum_{n=0}^{\infty} \sum_{m=-n}^{n} \widehat{u}_{nm} Y_{nm}(\theta, \varphi) \tag{2.3}$$

where

$$\widehat{u}_{nm} = \int_0^{\pi} \int_0^{2\pi} u(\theta, \varphi) Y_{nm}^*(\theta, \varphi) \sin \theta \, d\varphi \, d\theta \tag{2.4}$$

with Y_{nm}^* being the complex conjugate of Y_{nm}. Here, $Y_{nm}(\theta, \varphi)$ is a spherical harmonic of degree n (see [9]).

The solution of the Laplace equation in the unbounded domain Ω^c outside the oblate spheroid Γ_0 is given by

$$U(\mu, \theta, \varphi) = \sum_{n=0}^{\infty} \sum_{m=-n}^{n} \frac{T_n^m(\sinh \mu)}{T_n^m(\sinh \mu_0)} \widehat{u}_{nm} Y_{nm}(\theta, \varphi), \quad \mu \geq \mu_0 > 0. \tag{2.5}$$

Here T_n^m is given by

$$T_n^m = i \exp\left(\frac{i\pi n}{2} \right) Q_n^m(ix), \quad i^2 = -1,$$

where $Q_n^m(x)$ is the associated Legendre functions of the second kind (see [1], Chapter 8). Since

$$\left\| \frac{\partial \boldsymbol{x}}{\partial \mu}(\mu, \theta, \varphi) \right\| = f_0 \sqrt{\cosh^2 \mu - \sin^2 \theta},$$

the outward normal derivative $\partial_\nu U$ on Γ_0 can be computed as

$$\partial_\nu U(\theta, \varphi) = -\frac{1}{f_0 \sqrt{\cosh^2 \mu_0 - \sin^2 \theta}} \frac{\partial U}{\partial \mu}(\mu_0, \theta, \varphi)$$

Therefore the normal derivative of the solution on Γ_0 is

$$\partial_\nu U(\theta, \varphi) = -\frac{1}{f_0 \sqrt{\cosh^2 \mu_0 - \sin^2 \theta}} \sum_{n=0}^{\infty} \sum_{m=-n}^{n} \frac{\frac{dT_n^m}{d\mu}(\sinh \mu_0)}{T_n^m(\sinh \mu_0)} \widehat{u}_{nm} Y_{nm}(\theta, \varphi).$$

We denote by $\mathcal{K}$ the Dirichlet-to-Neumann map (Steklov-Poincaré operator) defined for any $v \in \mathcal{H}^{1/2}(\mathbb{S}^2)$ by

$$(\mathcal{K}v)(\theta, \varphi) := -\frac{1}{f_0 \sqrt{\cosh^2 \mu_0 - \sin^2 \theta}} \sum_{n=0}^{\infty} \sum_{m=-n}^{n} \frac{\frac{dT_n^m}{d\mu}(\sinh \mu_0)}{T_n^m(\sinh \mu_0)} \widehat{v}_{nm} Y_{nm}(\theta, \varphi). \quad (2.6)$$

It is known that (see e.g. [11]) (2.2) is equivalent to

$$\mathcal{K}u = g \quad \text{on} \quad \Gamma_0. \quad (2.7)$$

In subsequent sections, we will develop a Galerkin approximation method to u by first writing u as a solution of a pseudo-differential operator equation, defined by the Dirichlet-to-Neumann map (2.6). Using this approximation, together with (2.4) and (2.5), we will obtain an approximation to the solution U of the Neumann problem.

3. Weak formulation and Galerkin approximation

For a given real number s, the Sobolev space $\mathcal{H}^s(\Gamma_0)$ is defined by

$$\mathcal{H}^s(\Gamma_0) = \{ f \in \mathcal{D}'(\Gamma_0) : \|f\|^2_{\mathcal{H}^s(\Gamma_0)} = \sum_{n=0}^{\infty} \sum_{m=-n}^{n} (1 + n^2)^s |\widehat{f}_{nm}|^2 < \infty \},$$

where $\mathcal{D}'(\Gamma_0)$ is the set of all distributions defined on Γ_0.

Let us denote the usual $\mathcal{L}^2(\Gamma_0)$ inner product by $\langle \cdot, \cdot \rangle_{\Gamma_0}$. For two arbitrary functions $u, v \in \mathcal{H}^{1/2}(\Gamma_0)$, let us define the bilinear form

$$D(u, v) := \langle \mathcal{K}u, v \rangle_{\Gamma_0}.$$

Since the surface measure of Γ_0 is $ds = f_0^2 \cosh \mu_0 \sqrt{\cosh^2 \mu_0 - \sin^2 \theta} \sin \theta \, d\theta \, d\varphi$, from the definition of $D(u, v)$ we have

$$\begin{aligned} D(u, v) &= f_0^2 \cosh \mu_0 \int_0^{2\pi} \int_0^{\pi} (\mathcal{K}u) v \sqrt{\cosh^2 \mu_0 - \sin^2 \theta} \sin \theta \, d\theta \, d\varphi \\ &= f_0^2 \cosh \mu_0 \int_{\mathbb{S}^2} (\mathcal{K}u) v \sqrt{\cosh^2 \mu_0 - \sin^2 \theta} \, d\sigma, \end{aligned}$$

where $d\sigma = \sin \theta \, d\theta \, d\varphi$ is the surface measure on the unit sphere $\mathbb{S}^2$. Using (2.6) and the Plancherel theorem, we have

$$D(u, v) = -f_0 \sum_{n=0}^{\infty} \sum_{m=-n}^{n} \frac{dT_n^m(\sinh \mu_0)/d\mu}{T_n^m(\sinh \mu_0)} \cosh(\mu_0) \, \widehat{u}_{nm} \widehat{v}_{nm}^*.$$

Defining

$$G_n^m(x) := -\frac{(1 + x^2) \frac{d}{dx} T_n^m(x)}{T_n^m(x)} \tag{3.1}$$

so that

$$G_n^m(\sinh \mu) = -\frac{\frac{d}{d\mu} T_n^m(\sinh \mu)}{T_n^m(\sinh \mu)} \cosh \mu,$$

we can rewrite $D(u, v)$ as

$$D(u, v) = f_0 \sum_{n=0}^{\infty} \sum_{m=-n}^{n} G_n^m(\sinh \mu_0) \widehat{u}_{nm} \widehat{v}_{nm}^*. \tag{3.2}$$

By integrating (2.7) against test functions in $\mathcal{H}^{1/2}(\Gamma_0)$, we obtain the following weak formulation of the equation (2.7):

$$\text{Find } u \in \mathcal{H}^{1/2}(\Gamma_0) \text{ satisfying } D(u, v) = \langle g, v \rangle_{\Gamma_0} \quad \forall v \in \mathcal{H}^{1/2}(\Gamma_0). \tag{3.3}$$

The following result is proved in [6]:

Proposition 3.1. *The bilinear forms $D(\cdot,\cdot)$ is continuous and coercive on $\mathcal{H}^{1/2}(\Gamma_0)$, i.e., there exists constants C_1 and C_2 such that*

$$|D(u,v)| \le C_1 \|u\|_{\mathcal{H}^{1/2}(\Gamma_0)} \|v\|_{\mathcal{H}^{1/2}(\Gamma_0)} \quad \forall u, v \in \mathcal{H}^{1/2}(\Gamma_0)$$

and

$$C_2 \|v\|^2_{\mathcal{H}^{1/2}(\Gamma_0)} \le |D(v,v)| \quad \forall v \in \mathcal{H}^{1/2}(\Gamma_0)$$

So by using Lax–Milgram theorem, there exists a unique solution for the variational problem (3.3).

In the following we consider solving the Dirichlet-to-Neumann map approximately by the Galerkin method with radial basis functions as in [8] where we have considered the prolate spheroid. We obtain the Galerkin solution by mapping functions defined on the spheroid to functions defined on the sphere.

Since the approximate solution to (3.3) is sought in a finite dimensional subspace of $\mathcal{H}^{1/2}(\Gamma_0)$ on the oblate spheroid, we introduce the following bijection $\omega : \Gamma_0 \to \mathbb{S}^2$ to make use of the RBFs on the sphere,

$$\omega(\boldsymbol{x}) = (\sin\theta\cos\varphi, \sin\theta\sin\varphi, \cos\theta), \tag{3.4}$$

where $\boldsymbol{x}$ is an arbitrary point on Γ_0 with oblate spheroidal coordinates

$$\boldsymbol{x}(\theta,\varphi)=(f_0\cosh\mu_0\sin\theta\,\cos\varphi, f_0\,\cosh\mu_0\,\sin\theta\,\sin\varphi, f_0\,\sinh\mu_0\,\cos\theta). \tag{3.5}$$

Using this map, we define a kernel on Γ_0 as

$$\Psi(\boldsymbol{x},\boldsymbol{x}') = \Phi(\omega(\boldsymbol{x}),\omega(\boldsymbol{x}')), \quad \boldsymbol{x},\boldsymbol{x}' \in \Gamma_0 \tag{3.6}$$

where Φ is the strictly positive definite kernel defined on $\mathbb{S}^2$; see ([13, 17]).

The kernel Ψ can be expanded into a series of spherical harmonics as

$$\Psi(\boldsymbol{x},\boldsymbol{x}') = \sum_{n=0}^{\infty}\sum_{m=-n}^{n} \widehat{\phi}(n) Y_{nm}(\omega(\boldsymbol{x})) Y^*_{nm}(\omega(\boldsymbol{x}')). \tag{3.7}$$

For a set of scattered data points $X = \{\boldsymbol{x}_1, ..., \boldsymbol{x}_M\} \subset \Gamma_0$, we define V^τ by

$$V^\tau := \mathrm{span}\{\Psi_1, \cdots, \Psi_M\} \tag{3.8}$$

where $\Psi_j := \Psi(\boldsymbol{x}_j, \cdot)$, $j = 1, \ldots, M$. The solution of (3.3) is approximated by $u_X \in V^\tau$ satisfying

$$D(u_X, v) = \langle g, v\rangle_{\Gamma_0} \quad \forall v \in V^\tau. \tag{3.9}$$

To this end we have to solve a linear system

$$A\boldsymbol{c} = \boldsymbol{g} \tag{3.10}$$

where A is a matrix with entries $A_{i,j} = D(\Psi_i, \Psi_j), \quad i,j = 1,..,M$, and $\boldsymbol{g}$ is a vector with entries $g_j = \langle g, \Psi_j \rangle_{\Gamma_0}, \quad j = 1,..,M$. Using (3.2) and (3.7) we can write

$$A_{i,j} = f_0 \sum_{n=0}^{\infty} \sum_{m=-n}^{n} [\widehat{\phi}(n)]^2 G_n^m(\sinh \mu_0) Y_{nm}(\omega(\boldsymbol{x}_i)) Y_{nm}^*(\omega(\boldsymbol{x}_j)). \tag{3.11}$$

The positive definiteness of the matrix A is a direct consequence of coercivity of the bilinear form $D(\cdot,\cdot)$ established in Theorem 3.1. In the calculation we use a truncated version of $D(\cdot,\cdot)$ defined by

$$D_N(u,v) = f_0 \sum_{n=0}^{N} \sum_{m=-n}^{n} G_n^m(\sinh \mu_0) \widehat{u}_{nm} \widehat{v}_{nm}^*. \tag{3.12}$$

The matrix A is approximated by $A^{(N)}$ with entries

$$A_{i,j}^{(N)} = f_0 \sum_{n=0}^{N} \sum_{m=-n}^{n} [\widehat{\phi}(n)]^2 G_n^m(\sinh \mu_0) Y_{nm}(\omega(\boldsymbol{x}_i)) Y_{nm}^*(\omega(\boldsymbol{x}_j)).$$

We have to choose a sufficient large N ($N = N_{truncate} = 100$ or 120 are used in our numerical experiments) to guarantee the positive definiteness of the matrix $A^{(N)}$. This is termed a "variational" crime by Strang and Fix [14] and will be discussed later in the error analysis. The integral

$$\langle g, \Psi_j \rangle_{\Gamma_0} = f_0^2 \cosh \mu_0 \int_0^{\pi} \int_0^{2\pi} g(\theta,\varphi) \sqrt{\cosh^2 \mu_0 - \sin^2 \theta}\, \Psi_j(\theta,\varphi)\, \sin\theta \, d\varphi \, d\theta$$

can be evaluated by an appropriate cubature on the sphere $\mathbb{S}^2$ (e.g. [2]), or by using the Fourier expansion of g and Ψ_j.

Let $Y = \{\boldsymbol{y}_1, ..., \boldsymbol{y}_M\}$ be the image of X under the map ω, i.e. $\boldsymbol{y}_j = \omega(\boldsymbol{x}_j)$ for $j = 1, ..., M$. As Y is a set of scattered points on $\mathbb{S}^2$, we define the mesh norm h_Y of Y as usual,

$$h_Y = \sup_{\boldsymbol{y} \in \mathbb{S}^2} \min_{\boldsymbol{y}_j \in Y} \cos^{-1}(\boldsymbol{y} \cdot \boldsymbol{y}_j).$$

We also define the separation radius of the set Y by

$$q_Y = 0.5 \min_{\boldsymbol{y}_i \neq \boldsymbol{y}_j \in Y} \cos^{-1}(\boldsymbol{y} \cdot \boldsymbol{y}_j).$$

If $h_Y/q_Y \leq C$ for some universal constant C we called Y is a *quasi-uniform* set of points.

Similarly to [8, Theorem 3.2], we have the following approximation property for trial functions on the oblate spheroids. The proof carries over verbatim from Theorem 3.2 in [8], where one only has to substitute the map from the prolate to the sphere by the corresponding one of the oblate spheroid.

Proposition 3.2. *Assume that the Fourier-Legendre coefficients of the kernel Φ satisfy*

$$\widehat{\phi}(n) \simeq (1+n^2)^{-\tau} \tag{3.13}$$

holds for some $\tau > 1$. Let V^τ be defined as in (3.8)*. If $f \in \mathcal{H}^s(\Gamma_0)$, then for $t \leq \tau$, $t \leq s \leq 2\tau$ there exists $\eta \in V^\tau$ so that*

$$\|f - \eta\|_{\mathcal{H}^t(\Gamma_0)} \leq c h_Y^{s-t} \|f\|_{\mathcal{H}^s(\Gamma_0)},$$

where c is a positive constant independent of Y.

In (3.13) and henceforth, $a \simeq b$ means that there are two positive constants c_1 and c_2 so that $c_1 a \leq b \leq c_2 a$. Using Proposition 3.2 we will derive an error estimate for the approximation of the solution u of (3.3) by the solution u_X of (3.9).

Theorem 3.3. *Let V^τ be defined by (3.8) with Ψ satisfying (3.13) where $\tau > 1$. Assume that the solution u to (3.3) belongs to $\mathcal{H}^s(\Gamma_0)$ for some s satisfying $1/2 < s < 2\tau - 1$. Then there exists a positive constant C independent of the set X and an $N_0 > 0$ such that for all $N \geq N_0$ there holds*

$$\|u - u_X\|_{\mathcal{H}^{1/2}(\Gamma_0)} \leq C(h_Y^{s-1/2} + N^{-s+1/2}) \|u\|_{\mathcal{H}^s(\Gamma_0)}.$$

Proof. By using Strang Lemma [14], we have the following estimate

$$\|u - u_X\|_{\mathcal{H}^{1/2}(\Gamma_0)} \leq \inf_{v \in V^\tau} \|u - v\|_{\mathcal{H}^{1/2}(\Gamma_0)} + \max_{v \in V^\tau} \frac{|D_N(u,v) - D(u,v)|}{[D_N(v,v)]^{1/2}}. \tag{3.14}$$

The first term on the right-hand side can be estimated using Theorem 3.1

$$\inf_{v\in V^\tau} \|u-v\|_{\mathcal{H}^{1/2}(\Gamma_0)} \le c h_Y^{s-1/2} \|u\|_{\mathcal{H}^s(\Gamma_0)}. \tag{3.15}$$

To estimate the second term on the right-hand side, firstly we notice that it is shown in [6, Lemma 3.1] that

$$c(\mu_0)(n^2+1)^{1/2} < G_n^m(\sinh\mu_0) < C(\mu_0)(n^2+1)^{1/2}, \tag{3.16}$$

and that $G_n^{-m}(\sinh\mu_0) = G_n^m(\sinh\mu_0)$ for $0 \le m \le n$ and $n = 0, 1, 2 \ldots$.
By using the Cauchy-Schwarz inequality and (3.16) we have

$$\begin{aligned} |D_N(u,v) - D(u,v)| &= \left| f_0 \sum_{n=N+1}^{\infty} \sum_{m=-n}^{n} G_n^m(\sinh\mu_0) \widehat{u}_{nm} \widehat{v}_{nm}^* \right| \\ &\le C \left(\sum_{n=N+1}^{\infty} (n^2+1)^{\frac{1}{2}} |\widehat{u}_{nm}|^2 \right)^{\frac{1}{2}} \left(\sum_{n=N+1}^{\infty} (n^2+1)^{\frac{1}{2}} |\widehat{v}_{nm}|^2 \right)^{\frac{1}{2}}. \end{aligned}$$

It follows from

$$\sum_{n=N+1}^{\infty} (n^2+1)^{\frac{1}{2}} |\widehat{v}_{nm}|^2 \le (1+N^2)^{-s+1/2} \|v\|^2_{\mathcal{H}^s(\Gamma_0)} \quad \forall v \in \mathcal{H}^s(\Gamma_0),\ s > 1/2,$$

that

$$|D_N(u,v) - D(u,v)| \le C\,(1+N^2)^{-s+1/2} \|u\|_{\mathcal{H}^s(\Gamma_0)} \|v\|_{\mathcal{H}^s(\Gamma_0)}. \tag{3.17}$$

Using (3.16) again we have

$$D_N(v,v) = f_0 \sum_{n=0}^{N} \sum_{m=-n}^{n} G_n^m(\sinh\mu_0) |\widehat{v}_{nm}|^2 > c(\mu_0) \sum_{n=0}^{N} \sum_{m=-n}^{n} (n^2+1)^{1/2} |\widehat{v}_{nm}|^2.$$

Hence

$$\begin{aligned} D_N(v,v) &> c(\mu_0) \sum_{n=0}^{N} \sum_{m=-n}^{n} (n^2+1)^s (n^2+1)^{1/2-s} |\widehat{v}_{nm}|^2 \\ &\ge c(N^2+1)^{1/2-s} \sum_{n=0}^{N} \sum_{|m|\le n} (n^2+1)^s |\widehat{v}_{nm}|^2 \quad \text{for} \quad s > 1/2. \end{aligned} \tag{3.18}$$

Let

$$R_N := \sum_{n=0}^{N} \sum_{|m|\le n} (n^2+1)^s |\widehat{v}_{nm}|^2.$$

Since $v \in V^\tau$ we write v as $v = \sum_{i=1}^M \beta_i \Psi_i$. Hence $\widehat{v}_{nm} = \sum_{i=1}^M \beta_i (\widehat{\Psi}_i)_{nm}$. Note that

$$(\widehat{\Psi}_i)_{n,m} = |\widehat{\phi}(n)| Y_{nm}(\boldsymbol{x}_i). \tag{3.19}$$

Therefore

$$R_N = \sum_{n=0}^{N} (n^2+1)^s \sum_{i,j=1}^{M} \beta_i \beta_j |\widehat{\phi}(n)|^2 \sum_{m=-n}^{n} Y_{nm}(\boldsymbol{x}_i) Y_{nm}^*(\boldsymbol{x}_j).$$

By using the addition formula [9]

$$\sum_{m=-n}^{n} Y_{nm}(\boldsymbol{y}) Y_{nm}^*(\boldsymbol{z}) = \frac{2n+1}{4\pi} P_n(\boldsymbol{y}\cdot\boldsymbol{z}) \tag{3.20}$$

and (3.13) we deduce

$$R_N \simeq \sum_{n=0}^{N} (2n+1)(n^2+1)^{s-2\tau} \sum_{i,j=1}^{M} \beta_i \beta_j P_n(\boldsymbol{x}_i \cdot \boldsymbol{x}_j). \tag{3.21}$$

We need the following conjecture, which is strongly supported by our numerical experiments: for all $\epsilon > 1$, there exist $c > 0$ and $N_0 > 1$ such that for any set of *quasi-uniform* points $\{\boldsymbol{x}_1, \ldots, \boldsymbol{x}_M\}$, and any $\boldsymbol{\beta} = (\beta_1, \cdots, \beta_M) \in \mathbb{R}^M$, if $N \ge N_0$ there holds

$$\sum_{n\ge N+1} n^{-\epsilon} \sum_{i,j=1}^{M} \beta_i \beta_j P_n(\boldsymbol{x}_i \cdot \boldsymbol{x}_j) \le c \sum_{n=0}^{N} n^{-\epsilon} \sum_{i,j=1}^{M} \beta_i \beta_j P_n(\boldsymbol{x}_i \cdot \boldsymbol{x}_j). \tag{3.22}$$

The constant c is independent of the set X but N_0 may depend on the set X. The equivalent statement for (3.22) is that

$$\text{the matrix } cQ - R \text{ is positive-semidefinite,} \tag{3.23}$$

where Q and R are two $M \times M$ matrices with entries

$$Q_{i,j} = \sum_{n=0}^{N} n^{-\epsilon} P_n(\boldsymbol{x}_i \cdot \boldsymbol{x}_j), \quad R_{i,j} = \sum_{n\ge N+1} n^{-\epsilon} P_n(\boldsymbol{x}_i \cdot \boldsymbol{x}_j), \quad i,j = 1, \ldots, M.$$

We have carried out extensive numerical experiments to verify the conjecture. In particular, we computed the minimum eigenvalues of the matrix $100Q - R$ with $\epsilon = 1, 2, 3$ with up to 500 quasi-uniform points generated by Saff's algorithm [12]. The results are summarized in Figures 1–3. As can be seen from the figures, the minimum eigenvalues of the matrix $100Q - R$ with $\epsilon = 1, 2, 3$ are always positive.

By using (3.22) with $\epsilon = -1 - 2(s - 2\tau) > 1$ we deduce that for $N \geq N_0$

$$R_N \geq c \sum_{n=N+1}^{\infty} (2n+1)(n^2+1)^{s-2\tau} \sum_{i,j=1}^{M} \beta_i \beta_j P_n(\boldsymbol{x}_i \cdot \boldsymbol{x}_j). \tag{3.24}$$

It is then clear that

$$R_N \geq c||v||^2_{\mathcal{H}^s(\Gamma_0)}. \tag{3.25}$$

This together with (3.18) gives

$$D_N(v, v) = c(N^2+1)^{1/2-s}\|v\|^2_{\mathcal{H}^s(\Gamma_0)}. \tag{3.26}$$

Combining all the estimates in (3.17) and (3.26), we obtain

$$\max_{v \in V^\tau} \frac{|D_N(u, v) - D(u, v)|}{[D_N(v, v)]^{1/2}} \leq cN^{-s+1/2}\|u\|_{\mathcal{H}^s(\Gamma_0)}.$$

This together with (3.15) proves the assertion. □

4. Additive Schwarz preconditioners

The linear system (3.10) arising from the Galerkin approximation problem is usually ill-conditioned, especially when the separation radius of the set of scattered points is very small. In this situation, we propose a preconditioning algorithm based on the additive Schwarz operator, using a subspace decomposition of V^τ as

$$V^\tau = V_0 + \ldots + V_J$$

for some positive integer J. In the following, we will describe how to construct the subspaces V_j, for $j = 0, \ldots, J$.

Given a finite set of points $X = \{\boldsymbol{x}_1, \ldots, \boldsymbol{x}_M\}$ on the oblate spheroid Γ_0, we define the set Y on the sphere $\mathbb{S}^2$ to be the image of X via the map ω (cf. (3.4)), that is $Y = \{\boldsymbol{y}_1 = \omega(\boldsymbol{x}_1), \ldots, \boldsymbol{y}_M = \omega(\boldsymbol{x}_M)\}$.

We then decompose the set Y into J overlapping subsets Y_j for $j = 0, \ldots, J$ by the following simple algorithm:

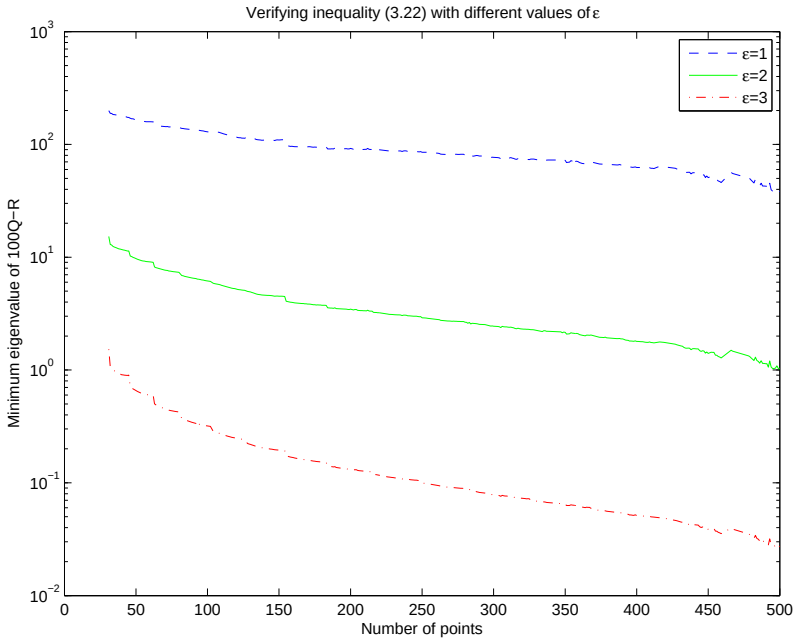

Figure 1: The minimum eigenvalues of the matrix $100Q - R$ with $N_0 = 40$ and $\epsilon = 1, 2, 3$.

Select $\alpha \in (0, \pi/3)$, $\beta \in (0, \pi]$;
$\boldsymbol{p}_1 = \boldsymbol{y}_1 \in Y$;
$Y_0 := \{\boldsymbol{p}_1\}$;
$Y_1 := \{\boldsymbol{y} \in Y : \cos^{-1}(\boldsymbol{y} \cdot \boldsymbol{p}_1) \leq \alpha\}$;
$J = 1, k = 1$;
while $Y_1 \cup \ldots \cup Y_k \neq Y$ **do**
  $k = k + 1$;
  $\boldsymbol{p}_k$ is chosen from $Y \backslash Y_0$ such that $\cos^{-1}(\boldsymbol{p}_{k-1} \cdot \boldsymbol{p}_k) \geq \beta$;
  $Y_0 := Y_0 \cup \{\boldsymbol{p}_k\}$;
  $Y_k := \{\boldsymbol{y} \in Y : \cos^{-1}(\boldsymbol{y} \cdot \boldsymbol{p}_k) \leq \alpha\ \}$;
end while
$J = k$

Roughly speaking, the algorithm selects from Y a coarse set of points $Y_0 = \{\boldsymbol{p}_1, \ldots, \boldsymbol{p}_J\}$ across the whole sphere so that the geodesic distance between any two successive points is not less than β. Then each set Y_k (for $k = 1, \ldots, J$) is a collection of points inside a spherical cap of radius α centered at $\boldsymbol{p}_k$. We note that the subsets Y_j may overlap. The subspaces V_j can

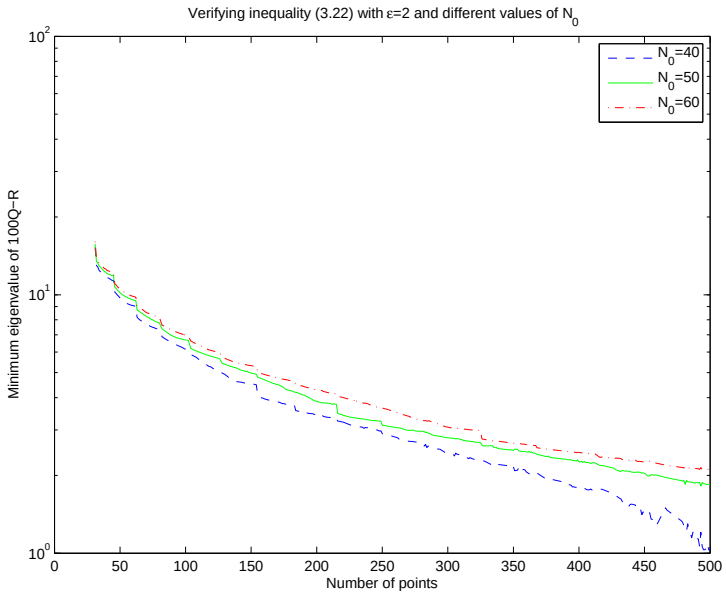

Figure 2: The minimum eigenvalues of the matrix $100Q - R$ with $\epsilon = 2$ and $N_0 = 40, 50, 60$

now be defined by

$$V_j = \text{span}\{\Psi_k = \Psi(\boldsymbol{y}_k, \cdot) : \boldsymbol{y}_k \in Y_j\}, \quad j = 0, \ldots, J.$$

Assume that functions in V_j have supports in Ω_j. We assume further that:

Assumption 4.1. *We can partition the index set* $\{1, \ldots, J\}$ *into* γ *(with* $1 \leq \gamma \leq J$*) sets* J_m*, for* $1 \leq m \leq \gamma$*, such that of* $i, j \in J_m$ *and* $i \neq j$ *then* $\Omega_i \cap \Omega_j = \emptyset$*.*

Let $P_j : V^\tau \to V_j$, $j = 0, \ldots, J$, be projections defined by

$$D(P_j v, w) = D(v, w) \quad \forall v \in V^\tau, \ \ \forall w \in V_j. \tag{4.1}$$

Then the additive Schwarz operator is defined by

$$P := P_0 + \cdots + P_J. \tag{4.2}$$

The additive Schwarz method for equation (3.9) consists of solving, by an iterative method, the equation

$$P\widetilde{u} = g, \tag{4.3}$$

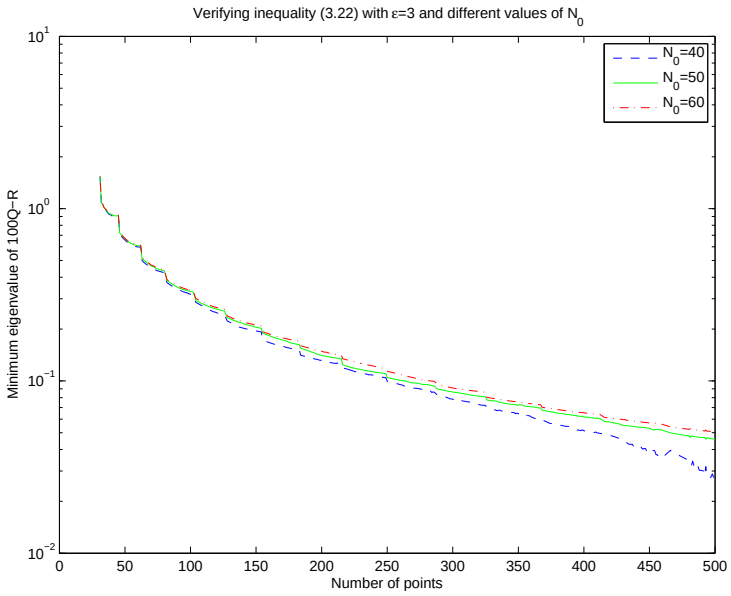

Figure 3: The minimum eigenvalues of the matrix $100Q - R$ with $\epsilon = 3$ and $N_0 = 40, 50, 60$

where the right-hand side is given by $g = \sum_{j=0}^{J} g_j$, with $g_j \in V_j$ being solutions of

$$D(g_j, w) = \int_{\Gamma_0} f w ds, \quad \text{for any } w \in V_j.$$

Solving (4.3) is equivalent to solving (3.9), and in turn equivalent to solving

$$P_j \widetilde{u} = g_j, \quad j = 0, \ldots, J.$$

The operator P can be considered as the preconditioned version of $\mathcal{K}$, i.e. $P = B\mathcal{K}$ for some preconditioner B. The preconditioning technique is in practice performed by computing the action of B^{-1} on a residual $r \in V^\tau$. This consists of the solution of independent problems on each of the subspaces involved in the decomposition.

1. Correction on the global coarse set Y_0:

$$\text{Find } u_0 \in V_0 \text{ satisfying} \quad D(u_0, v) = \int_{\Gamma_0} r v ds \quad \forall v \in V_0.$$

2. Corrections on the local sets Y_j, $j = 1, \ldots, J$:

$$\text{Find } u_j \in V_j \text{ satisfying} \quad D(u_j, v) = \int_{\Gamma_0} rv ds \quad \forall v \in V_j.$$

3. The residual r in the conjugate gradient is preconditioned by:

$$B^{-1}r := \sum_{j=0}^{J} u_j.$$

For the implementation details, see the pseudocode in [7, page 17].

By noting (3.1), the symbol of the operator $\mathcal{K}$ defined in (2.6) behaves like $(n^2+1)^{1/2}$, see (3.16), i.e. $\mathcal{K}$ is a pseudodifferential operator of order 1. This allows us to extend our analysis [15] for the overlapping Schwarz preconditioner on the sphere to the prolate spheroid.

Lemma 4.2. *1. Under Assumption 4.1, there exists a positive constant c independent of the set X such that for every $v \in V^\tau$ satisfying $v = \sum_{j=0}^{J} v_j$ with $v_j \in V_j$ for $j = 0, \ldots, J$ there holds*

$$D(v, v) \leq c\gamma \sum_{j=0}^{J} D(v_j, v_j).$$

2. For any $u \in V^\tau$ there exist $u_j \in V_j$, $j = 0, \ldots, J$, satisfying $u = \sum_{j=0}^{J} u_j$ and

$$\sum_{j=0}^{J} D(u_j, u_j) \leq \left(1 + \frac{J}{(1 - \|\widetilde{Q}\|_D)^2}\right) D(u, u),$$

where $\widetilde{Q} = Q_J \cdots Q_1$. Here Q_i is the orthogonal projection from V^τ onto $V_i^\perp$, the orthogonal complement of V_i with respect to the inner product induced by the bilinear form $D(\cdot, \cdot)$.

Proof. By using the map ω (cf. (3.4)) from the oblate spheroid to the sphere, for any function $f \in \mathcal{H}^{1/2}(\Gamma_0)$, if $F = f(\omega^{-1}\boldsymbol{y})$ then F is a function in $\mathcal{H}^{1/2}(\mathbb{S}^2)$. Using this, we can carry over the proof of [15, Lemma 4.4 and Lemma 4.8] for the functions defined on the sphere here. □

As a consequence of the previous lemma, we obtain the following bound for the condition number of the Schwarz operator.

Theorem 4.3. *The condition number of the additive Schwarz operator P is bounded by*

$$\kappa(P) \leq c\gamma \left(1 + \frac{J}{(1 - \|\widetilde{Q}\|_D)^2}\right).$$

where c is a constant independent of γ and the set X.

5. Implementation of the Galerkin method

In order to compute the entries A_{ij} of the stiffness matrix given in (3.10), we need to compute the spherical harmonics Y_{nm} and the functions G_n^m; see (3.11).

The spherical harmonics are computed by using the formula [1]

$$Y_{nm}(\theta, \varphi) := \sqrt{\frac{2n+1}{4\pi}} P_n^{|m|}(\cos\theta) e^{im\varphi}, \tag{5.1}$$

where $P_n^m(x)$ are associated Legendre functions of the first kind which can be computed using the following recurrence relations, for $m = 0, 1, 2, ..., n$ and $n = 0, 1, 2, ...$

$$\begin{aligned} P_n^n(x) &= \frac{\sqrt{(2n)!}}{2^n n!}(1 - x^2)^{n/2}, \\ P_{n-1}^n(x) &= 0, \\ P_{n+1}^m(x) &= v_n^m x P_n^m(x) + w_n^m P_{n-1}^m(x), \end{aligned}$$

where

$$v_n^m = \frac{(2n+1)}{\sqrt{(n-m+1)(n+m+1)}} \quad \text{and} \quad w_n^m = \frac{\sqrt{(n-m)(n+m)}}{\sqrt{(n-m+1)(n+m+1)}}.$$

The functions T_n^m given by

$$T_n^m(x) = i \exp\left(\frac{i\pi n}{2}\right) Q_n^m(ix) \tag{5.2}$$

are calculated using the algorithm for oblate spheroidal harmonics presented in (see [4]).

In order to calculate $\frac{d}{dx}T_n^m$ we use (5.2). We have

$$Q_{n+1}^m(ix) = -i\exp(-\frac{i\pi(n+1)}{2})T_{n+1}^m(x) \text{ and } Q_n^m(ix) = -i\exp(-\frac{i\pi n}{2})T_n^m(x).$$

Thus

$$\frac{Q_{n+1}^m(ix)}{Q_n^m(ix)} = -i\frac{T_{n+1}^m(x)}{T_n^m(x)} \tag{5.3}$$

and with

$$\frac{d}{dx}T_n^m(x) = -\exp\big(\frac{i\pi n}{2}\big)\frac{d}{dz}Q_n^m(ix) \quad (z = ix)$$

we finally obtain

$$\frac{\frac{d}{dx}T_n^m(x)}{T_n^m(x)} = \frac{-\exp\big(\frac{i\pi n}{2}\big)\frac{d}{dz}Q_n^m(ix)}{i\exp\big(\frac{i\pi n}{2}\big)Q_n^m(ix)} = i\frac{\frac{d}{dz}Q_n^m(ix)}{Q_n^m(ix)}. \tag{5.4}$$

Furthermore, it is known that (see [6])

$$-i\frac{\frac{d}{dz}Q_n^m(z)}{Q_n^m(z)}(1-z^2) = (n+1)(-iz) + (n-m+1)\frac{iQ_{n+1}^m(z)}{Q_n^m(z)} \tag{5.5}$$

and comparing (5.4) and (5.5) (with $z = ix \Longrightarrow (1-z^2) = (1+x^2)$) we have

$$\begin{aligned} -(1+x^2)\frac{\frac{d}{dx}T_n^m(x)}{T_n^m(x)} &= -i\frac{\frac{d}{dz}Q_n^m(z)}{Q_n^m(z)}(1-z^2) \\ &= (n+1)(-iz) + (n-m+1)\frac{iQ_{n+1}^m(z)}{Q_n^m(z)}. \end{aligned}$$

Therefore the recurrence relation (with $iz = x$ and (5.3)) for $\frac{d}{dx}T_n^m$ can be expressed as

$$-(1+x^2)\frac{\frac{d}{dx}T_n^m(x)}{T_n^m(x)} = (n+1)x + (n-m+1)\frac{T_{n+1}^m(x)}{T_n^m(x)}. \tag{5.6}$$

With this relation the term $G_n^m(\sinh\mu_0)$ in the entry A_{ij} of the stiffness matrix (see 3.11) and (3.1) can be computed by using the relation

$$G_n^m(x) = (n+1)x + (n-m+1)\frac{T_{n+1}^m(x)}{T_n^m(x)}, \quad m = 0,1,\ldots,n; n = 0,1,2,\ldots$$

For negative values of m we use the relation $G_n^m(x) = G_n^{-m}(x)$.

The right hand side terms g_j are computed by using the Fourier coefficients of g and Φ_j and Parseval's identity.

In our experiments, we use the kernel $\Psi(\boldsymbol{x}, \boldsymbol{x}') = \Phi(\omega(\boldsymbol{x}), \omega(\boldsymbol{x}'))$ where for arbitrary $\boldsymbol{y}, \boldsymbol{z} \in \mathbb{S}^2$,

$$\Phi(\boldsymbol{y}, \boldsymbol{z}) = \rho_m(\sqrt{2 - 2\boldsymbol{y} \cdot \boldsymbol{z}})$$

with ρ_m being locally supported radial basis functions defined by Wendland [16]; see Table 1. It is shown by Narcowich and Ward [10] that in this case (3.13) holds for $\tau = m + 3/2$.

m	$\rho_m(r)$	τ
0	$(1-r)_+^2$	1.5
1	$(1-r)_+^4(4r+1)$	2.5
2	$(1-r)_+^6(35r^2+18r+3)$	3.5

Table 1: Wendland's RBFs

6. Numerical experiments

In our experiments we choose the oblate spheroid Γ_0 such that $f_0 = 4$ and $\mu_0 = 1$. Let the Neumann condition be

$$g(\mu, \theta, \varphi) = -\frac{\sinh\mu \sin\theta \cos\varphi (2\cosh^2\mu + \cos^2\theta)}{f_0^2(\cosh^2\mu - \cos^2\theta)^{\frac{5}{2}}}$$

so that the exact solution to (2.2) is

$$U(\mu, \theta, \varphi) = \frac{\cosh\mu \sin\theta \cos\varphi}{f_0^2(\cosh^2\mu - \cos^2\theta)^{\frac{3}{2}}}. \tag{6.1}$$

This example is taken from [6] where the authors solve (3.3) using piecewise bilinear functions on grids of $\Lambda = \{(\theta, \varphi) : 0 \le \theta \le \pi, 0 \le \varphi \le 2\pi\}$.

We solved (3.9) in the space V^τ defined in (3.8) with three different types of sets of points X.

Points of type 1. As in [6], we divide the intervals $[0, \pi]$ and $[0, 2\pi]$ into N_1 and N_2 subintervals, respectively, by

$$\theta_s = s\pi/N_1, \quad s = 0, 1, 2, ..., N_1$$

and

$$\varphi_t = 2t\pi/N_2, \quad t = 0, 1, 2, ..., N_2.$$

Then we use $M := N_2(N_1 - 1)$ points on Γ_0,

$$\boldsymbol{x}_{(N_2-1)s+t} = (f_0 \cosh\mu_0 \sin\theta_s \cos\varphi_t, f_0 \cosh\mu_0 \sin\theta_s \sin\varphi_t, f_0 \sinh\mu_0 \cos\theta_s),$$

where $1 \le s \le N_1 - 1$ and $1 \le t \le N_2$ to construct the basis functions.

Points of type 2. Next, we generate sets of points X on Γ_0 as images under the mapping ω, see (3.4), of sets of points $Y = \{\boldsymbol{y}_1, ..., \boldsymbol{y}_M\}$ on $\mathbb{S}^2$ which are defined by using Saff's algorithm [12]. This algorithm partitions $\mathbb{S}^2$ into M equal-area regions whose center are $\boldsymbol{y}_1, ..., \boldsymbol{y}_M$; see Figure **??**.

Points of type 3. Finally, we use sets of scattered points on the oblate spheroid which are obtained by mapping to the oblate spheroid the geocentric coordinates of data points taken from MAGSAT satellite data; see Figure 4. These sets are extracted from a full data set of about 26 million points in such a way that the separation radius of each set $q_Y = \frac{1}{2} \min_{\boldsymbol{y} \ne \boldsymbol{y}'} \cos^{-1}(\boldsymbol{y} \cdot \boldsymbol{y}')$ is not too small; see Table 6.

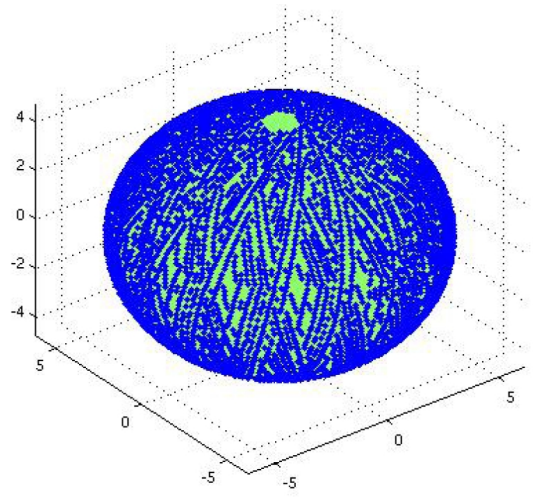

Figure 4: Image of satellite points on the oblate spheroid

We solved the matrix equation (3.10) by the conjugate gradient method with relative tolerance 10^{-10}, i.e. the stopping criteria is

$$\frac{\|A\boldsymbol{c}^{(m)} - \boldsymbol{g}\|_{l^2}}{\|\boldsymbol{g}\|_{l^2}} \le 10^{-10}. \tag{6.2}$$

Here $\boldsymbol{c}^{(m)}$ is the mth iterate.

Let $e := u - u_X$ where $u(\theta, \varphi) = U(\mu_0, \theta, \varphi)$, see (6.1), is the solution to (3.3) and u_X is the solution to (3.9). We compute $\|e\|_{\mathcal{L}^2(\Gamma_0)}$ and $\|e\|_{\mathcal{H}^{1/2}(\Gamma_0)}$ approximately by

$$\|e\|_{\mathcal{L}^2(\Gamma_0)} \approx \left(\sum_{n=0}^{120} \sum_{m=-n}^{n} |\widehat{(u_X)}_{nm} - \widehat{u}_{nm}|^2 \right)^{1/2}$$

and

$$\|e\|_{\mathcal{H}^{1/2}(\Gamma_0)} \approx \left(\sum_{n=0}^{120} (1+n^2)^{1/2} \sum_{m=-n}^{n} |\widehat{(u_X)}_{nm} - \widehat{u}_{nm}|^2 \right)^{1/2}$$

in which

$$\widehat{(u_X)}_{nm} = \sum_{i=1}^{M} \widehat{\phi}(n) c_i Y_{nm}(\omega(\boldsymbol{x}_i))$$

and $\hat{u}_{nm}$ is computed by using a quadrature [2] for formula (2.4).

We also compute l_2 and l_∞ errors for point sets of type 1. Let $\mathcal{G}$ be points of the grid of size $(N_1, N_2) = (160, 320)$, then

$$\|e\|_{l^\infty(\Gamma_0)} = \max_{y \in \mathcal{G}} |u_X(y) - u(y)|$$

and

$$\|e\|_{l^2(\Gamma_0)} = \left(\frac{1}{|\mathcal{G}|} \sum_{y \in \mathcal{G}} |u_X(y) - u(y)|^2 \right)^{1/2}$$

where $|\mathcal{G}| = 50880$ is cardinality of $\mathcal{G}$ and $|\mathcal{G}| := N_2(N_1 - 1)$.

Table 2 shows the experimental orders of convergence (EOC) for the errors in the $\mathcal{H}^{1/2}(\Gamma_0)$-norm (energy norm) when Saff points (points of type 2) are used.

The numbers in the Tables 3, 4 and 5 show fast convergence of our RBF Galerkin method applied to the Dirichlet-to-Neumann map with different values of N on different grids of size (N_1, N_2).

Table 6 gives the errors in the $\mathcal{L}^2(\Gamma_0)$ and $\mathcal{H}^{1/2}(\Gamma_0)$ norms for scattered points (points of type 3). In this case, the matrix is ill conditioned and hence

a preconditioner is required. Table 7 shows the corresponding numbers of iteration of the preconditioned conjugate gradient using the same stopping criteria as before, i.e. with the relative tolerance $\leq 10^{-10}$. Errors of the same order as in the non-preconditioned case are obtained. The advantage of the preconditioner can be observed.

Acknowledgement

The paper was written while Costea and Stephan were visiting the University of New South Wales and Tran was visiting Leibniz University of Hannover. These authors would like to thank the host universities for their supports. Le Gia was supported by the School of Mathematics and Statistics (UNSW) and the Australian Research Council under its Centres of Excellence Program. Costea and Stephan would also like to acknowledge the financial support provided by the Excellence Cluster Quest (Centre for Quantum Engineering and Space-Time Research), Leibniz University of Hannover.

m	N_1	N_2	$\|e\|_{\mathcal{L}^2(\Gamma_0)}$	$\|e\|_{\mathcal{H}^{1/2}(\Gamma_0)}$	$\|e\|_{l^2(\Gamma_0)}$	$\|e\|_{l^\infty(\Gamma_0)}$
0	10	20	0.3854E-03	0.1779E-02	0.1028E-03	0.6957E-03
0	20	40	0.4949E-04	0.3248E-03	0.1343E-04	0.9091E-04
0	40	80	0.5814E-05	0.5303E-04	0.1888E-05	0.1116E-04
0	80	160	0.2402E-08	0.2470E-07	0.4065E-06	0.1425E-05
1	10	20	0.1033E-03	0.4509E-03	0.2828E-04	0.1099E-03
1	20	40	0.2922E-05	0.1848E-04	0.7933E-06	0.3357E-05
1	40	80	0.9079E-07	0.8163E-06	0.2402E-07	0.1068E-06
1	80	160	0.8770E-09	0.5410E-08	0.1235E-08	0.4930E-08
2	10	20	0.6982E-04	0.2818E-03	0.2356E-04	0.6829E-04
2	20	40	0.4338E-06	0.2695E-05	0.1310E-06	0.4398E-06
2	40	80	0.3392E-08	0.2924E-07	0.1089E-08	0.4647E-08
2	80	160	0.1155E-08	0.6304E-08	0.6819E-09	0.4083E-08

Table 3: Errors on grid points, using conjugate gradient method for $N_{truncate} = 80$

m	M	h_X	$\mathcal{H}^{1/2}err$	EOC
0	100	0.2672	3.1112E-03	
	200	0.1942	1.3158E-03	2.70
	500	0.1237	3.9392E-04	2.67
	1000	0.0849	1.6113E-04	2.38
	2000	0.0609	6.7877E-05	2.60
	4000	0.0426	2.4877E-05	2.81
1	100	0.2672	1.0988E-03	
	200	0.1942	1.9053E-04	5.49
	500	0.1237	2.4204E-05	4.57
	1000	0.0849	4.7746E-06	4.31
	2000	0.0609	9.9207E-07	4.73
	4000	0.0426	1.9228E-07	4.59
2	100	0.2672	1.1860E-03	
	200	0.1942	8.0785E-05	8.42
	500	0.1237	3.6622E-06	6.86
	1000	0.0849	3.3840E-07	6.33
	2000	0.0609	3.6577E-08	6.70
	4000	0.0426	3.5598E-09	6.52

Table 2: Errors with Saff points and $\rho_m(r)$

m	N_1	N_2	$\|e\|_{\mathcal{L}^2(\Gamma_0)}$	$\|e\|_{\mathcal{H}^{1/2}(\Gamma_0)}$	$\|e\|_{l^2(\Gamma_0)}$	$\|e\|_{l^\infty(\Gamma_0)}$
0	10	20	0.3854E-03	0.1779E-02	0.1028E-03	0.6957E-03
0	20	40	0.4949E-04	0.3248E-03	0.1343E-04	0.9092E-04
0	40	80	0.5814E-05	0.5303E-04	0.1889E-05	0.1114E-04
0	80	160	0.2407E-08	0.2463E-07	0.4065E-06	0.1425E-05
1	10	20	0.1033E-03	0.4509E-03	0.2828E-04	0.1099E-03
1	20	40	0.2922E-05	0.1848E-04	0.7933E-06	0.3357E-05
1	40	80	0.9079E-07	0.8163E-06	0.2402E-07	0.1068E-06
1	80	160	0.8768E-09	0.5410E-08	0.1235E-08	0.4936E-08
2	10	20	0.6982E-04	0.2818E-03	0.2356E-04	0.6829E-04
2	20	40	0.4338E-06	0.2695E-05	0.1310E-06	0.4398E-06
2	40	80	0.3393E-08	0.2924E-07	0.1090E-08	0.4659E-08
2	80	160	0.1153E-08	0.6296E-08	0.6811E-09	0.4094E-08

Table 4: Errors on grid points, using conjugate gradient method for $N_{truncate} = 100$

m	N_1	N_2	$\|e\|_{\mathcal{L}^2(\Gamma_0)}$	$\|e\|_{\mathcal{H}^{1/2}(\Gamma_0)}$	$\|e\|_{l^2(\Gamma_0)}$	$\|e\|_{l^\infty(\Gamma_0)}$
0	10	20	0.3854E-03	0.1779E-02	0.1028E-03	0.6957E-03
0	20	40	0.4949E-04	0.3248E-03	0.1343E-04	0.9093E-04
0	40	80	0.5814E-05	0.5303E-04	0.1889E-05	0.1114E-04
0	80	160	0.2391E-08	0.2437E-07	0.4065E-06	0.1425E-05
1	10	20	0.1033E-03	0.4509E-03	0.2828E-04	0.1099E-03
1	20	40	0.2922E-05	0.1848E-04	0.7933E-06	0.3357E-05
1	40	80	0.9079E-07	0.8163E-06	0.2402E-07	0.1068E-06
1	80	160	0.8743E-09	0.5401E-08	0.1234E-08	0.4908E-08
2	10	20	0.6982E-04	0.2818E-03	0.2356E-04	0.6829E-04
2	20	40	0.4338E-06	0.2695E-05	0.1310E-06	0.4397E-06
2	40	80	0.3392E-08	0.2924E-07	0.1090E-08	0.4640E-08
2	80	160	0.1155E-08	0.6304E-08	0.6818E-09	0.4100E-08

Table 5: Errors on grid points, using conjugate gradient method for $N_{truncate} = 120$

M	q_Y	$\|e\|_{\mathcal{L}^2(\Gamma_0)}$	$\|e\|_{\mathcal{H}^{1/2}(\Gamma_0)}$	ITER	CPU
3470	$\pi/140$	6.25503E-006	5.01114E-005	2809	234.6
7763	$\pi/200$	2.41695E-006	2.13257E-005	27064	13323.7
10443	$\pi/240$	1.87142E-006	1.62031E-005	30931	17361.9

Table 6: Computational time in seconds (CPU), number of conjugate gradient iterations (ITER) and errors for scattered points from MAGSAT for $N_{truncate} = 100$ and $\rho_0(r)$

M	$\cos\alpha$	$\cos\beta$	$\|e\|_{\mathcal{L}^2(\Gamma_0)}$	$\|e\|_{\mathcal{H}^{1/2}(\Gamma_0)}$	ITER	CPU
3470	0.9	-0.15500000	6.24283E-006	5.02580E-005	73	4.3
7763	0.97	0.99999996	2.41695E-006	2.13257E-005	939	294.1
10443	0.98	0.99999996	1.87142E-006	1.62031E-005	1602	1085.8

Table 7: Computational time in seconds (CPU), number of iterations (ITER) for overlapping additive Schwarz preconditioner and errors for scattered points from MAGSAT for $N_{truncate} = 100$ and $\rho_0(r)$

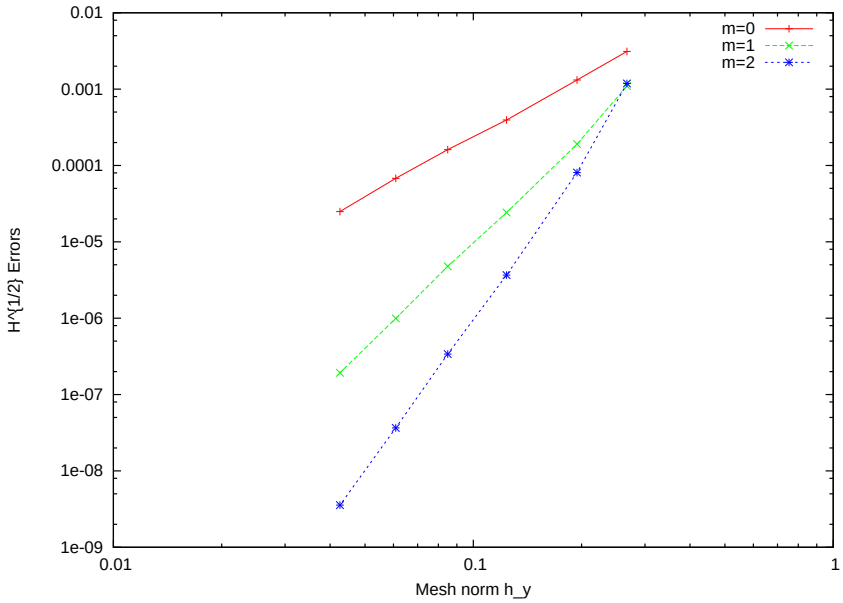

Figure 5: Log-log plot for $\mathcal{H}^{1/2}(\Gamma_0)$ errors using Wendland RBFs $\rho_m(r)$

References

[1] M. Abramowitz, I. Stegun, Handbook of Mathematical Functions with Formulas, Graphs, and Mathematical Tables, Denver, New York, 1965.

[2] J. R. Driscoll, D. M. Healy, Computing Fourier transforms and convolutions on the 2-sphere, Adv. in Applied Math. 15 (1994) 202–250.

[3] W. Freeden, T. Gervens, M. Schreiner, Constructive Approximation on the Sphere with Applications to Geomathematics, Oxford University Press, Oxford, 1998.

[4] A. Gil, J. Segura, A code to evaluate prolate and oblate spheroidal harmonics, Computer Physics Communications 108 (1998) 267–278.

[5] E. W. Grafarend, F. W. Krumm, V. S. Schwarze (eds.), Geodesy: the Challenge of the 3rd Millennium, Springer, Berlin, 2003 (2003).

[6] H.-y. Huang, D.-h. Yu, The ellipsoid artificial boundary method for three-dimensional unbounded domains, J. Comput. Math. 27 (2-3) (2009) 196–214.

[7] Q. T. Le Gia, I. H. Sloan, T. Tran, Overlapping additive Schwarz preconditioners for elliptic PDEs on the unit sphere, Math. Comp. 78 (2009) 79–101.

[8] Q. T. .Le Gia, T. Tran, E. Stephan, Solution to the Neumann problem exterior to a prolate spheroid by radial basis functions, Advances in Comp. Math. 34 (2011) 83–103.

[9] C. Müller, Spherical Harmonics, vol. 17 of Lecture Notes in Mathematics, Springer-Verlag, Berlin, 1966.

[10] F. J. Narcowich, J. D. Ward, Scattered data interpolation on spheres: error estimates and locally supported basis functions, SIAM J. Math. Anal. 33 (2002) 1393–1410.

[11] J.-C. Nédélec, Acoustic and Electromagnetic Equations, Springer-Verlag, New York, 2000.

[12] E. B. Saff, A. B. J. Kuijlaars, Distributing many points on a sphere, Math. Intelligencer 19 (1997) 5–11.

[13] I. J. Schoenberg, Positive definite function on spheres, Duke Math. J. 9 (1942) 96–108.

[14] G. Strang, G. Fix, An Analysis of the Finite Element Method, Prentice-Hall, Englewood Cliffs, New Jersey, 1973.

[15] T. Tran, Q. T. Le Gia, I. H. Sloan, E. P. Stephan, Preconditioners for pseudodifferential equations on the sphere with radial basis functions, Numer. Math. 115 (2009) 141–163, available online: http://dx.doi.org/10.1007/s00211-009-0269-8.

[16] H. Wendland, Scattered Data Approximation, Cambridge University Press, Cambridge, 2005.

[17] Y. Xu, E. W. Cheney, Strictly positive definite functions on spheres, Proc. Amer. Math. Soc. 116 (1992) 977–981.